A water-soluble perylene derivative for live-cell imaging

Yongshan MA[1,*], Fengxia ZHANG[2], Jinfeng ZHANG[1], Tianyi JIANG[1]

[1]School of Municipal and Environmental Engineering, Shandong Jianzhu University, Jinan, P.R. China
[2]Shandong Provincial Key Laboratory of Metrology and Measurement, Shandong Institute of Metrology,
Shandong Social Justice Institute of Metrology, Jinan, P.R. China

Abstract: Glutamic functionalized water-soluble perylene diimide, N, N'-di (L-glutamic amine)-perylene-3,4,9,10-tetracarboxylic diimide (GAPTCD) has three absorbance maxima at 469, 498, and 534 nm and two emission peaks at 550 and 587 nm. Owing to the highly negative electrostatic potential of the perylene plane, the perylene derivative showed good water solubility and strong fluorescence in alkali and neutral solutions. Both the absorbance and emission intensities decreased with the decreasing of pH from 9.66 to 5.92. This could be ascribed to the $\pi - \pi$ stacking produced by H^+ at the carboxyl group due to its electron accepting nature. Electrostatic potential maps also indicated that GAPTCD can exist stably in basic to weak acidic aqueous solution. Then GAPTCD was successfully applied as a high performance fluorochrome for imaging of living hela cells.

Key words: Water-soluble perylene derivative, fluorescence spectrum, absorption spectrum, map calculations, living cell staining

1. Introduction

Recently, fluorescent dyes for living cells staining based on water-soluble perylene diimide (PDI) derivatives have attracted considerable interest because of their high fluorescence quantum yields and outstanding photochemical stabilities.[1−5] PDIs are chromophores that exhibit high fluorescence quantum yields close to unity[6,7] and the photostability of the PDI fluorophores is significantly higher than that of other available fluorophores.[8] However, PDIs display low solubility in aqueous media because of aggregation of perylene chromophores.[9−11] To increase the solubility of PDIs, additional ionic side groups have been introduced directly at the imide position or on the perylene core.[12] In particular, the former strategy using an ionic substituent could improve the solubility of PDIs in solvents without changing their photophysical properties significantly.[13,14] Recently, Proença and coworkers reported a set of highly water-soluble PDIs with outstanding fluorescence quantum yields in water.[15] Gao and coworkers reported water-soluble dendritic perylene bisimide probes with triblock structures and these probes have been proven to be cell-permeable and could be used for living cell imaging.[16] They prepared the probes with triblock structures: PDI moieties as fluorescence cores, glutamic acid as scaffolds for suppressing aggregation of the central PDI chromophores, and polyethylene glycol chains as hydrophilic shells for reducing cytotoxicity and inducing water solubility. The aggregation of the PDI must be suppressed by large bulky dendritic polyethylene glycol groups and the probes were synthesized by multistepwise coupling reactions with perylene tetracarboxylic acid bisanhydride, L-aspartic acid, and 2,5,8,12,15,18-hexaoxa-10-nonadecanamine.

*Correspondence: mlosh@sdjzu.edu.cn

However, some reactions were not easy to carry out and so simple and easily synthesized PDI probes for living cells staining remain rare. Only a limited number of PDI probes have been reported to be practical for living cell imaging, and each of them had its own disadvantages including high cytotoxicity, low fluorescence quantum yields, or photobleaching.[17] Therefore, low cytotoxicity PDIs with high fluorescence in aqueous medium are highly desired.[18]

In the present study, glutamic functionalized water-soluble perylene diimide, N, N'-di (L-glutamic amine)-perylene-3,4,9,10-tetracarboxylic diimide (GAPTCD) (Scheme) was synthesized and used for living cell imaging.

2. Results and discussion

2.1. Optical properties

2.1.1. UV-visible spectra of GAPTCD

The existence form as well as the spectra of GAPTCD depended on pH. GAPTCD displayed good solubility in alkali solutions due to the electrostatic repulsion between its multiple negative charges. PDIs had a strong aggregation tendency that would change their absorption spectra. Figure 1a shows the pH-dependent absorption spectra of GAPTCD (10^{-5} M) in water. The spectra showed two absorption bands (534 nm, 498 nm) and a broad shoulder peak around 469 nm, which corresponded to the characteristics of the $0-0$, 1, and 2 transitions.[9] As free monomers, the normal progression of Franck–Condon factors was $A^{0-0} > A^{0-1} > A^{0-2}$. However, when the monomers began to aggregate, increased 0–1 and 0–2 transitions were observed.[20]

Both of the main peaks decreased along with the pH value decrease from 10.75 to 3.97. Figure 1b shows the normalized spectra at $0-0$ transition. The A^{0-1}/A^{0-0} of GAPTCD slightly increased with the decrease in pH from 10.75 to 5.92 and then increased quickly from pH 5.12 to 3.97. It indicated that the negative charges in the glutamic amine moiety disfavor aggregation forms of GAPTCD. Compared with the absorption band of 534 nm at pH 10.75, it is red-shifted to 539 nm at pH 3.97. This could be ascribed to $\pi - \pi$ stacking produced by H^+ at the carboxyl group due to its electron accepting nature. In this case, most of the monomers aggregated together and then prevented light transmission instead of absorption. These data suggested that GAPTCD can exist stably in alkali and neutral aqueous solution.
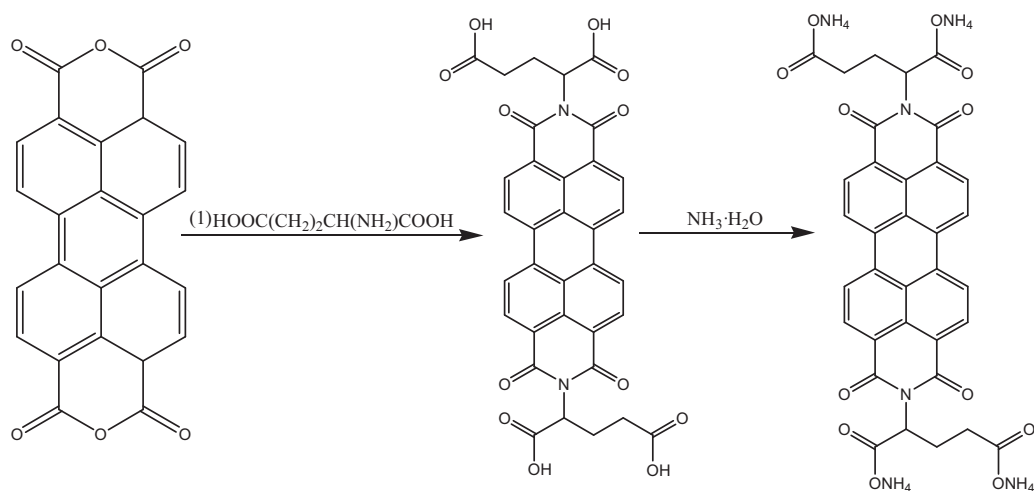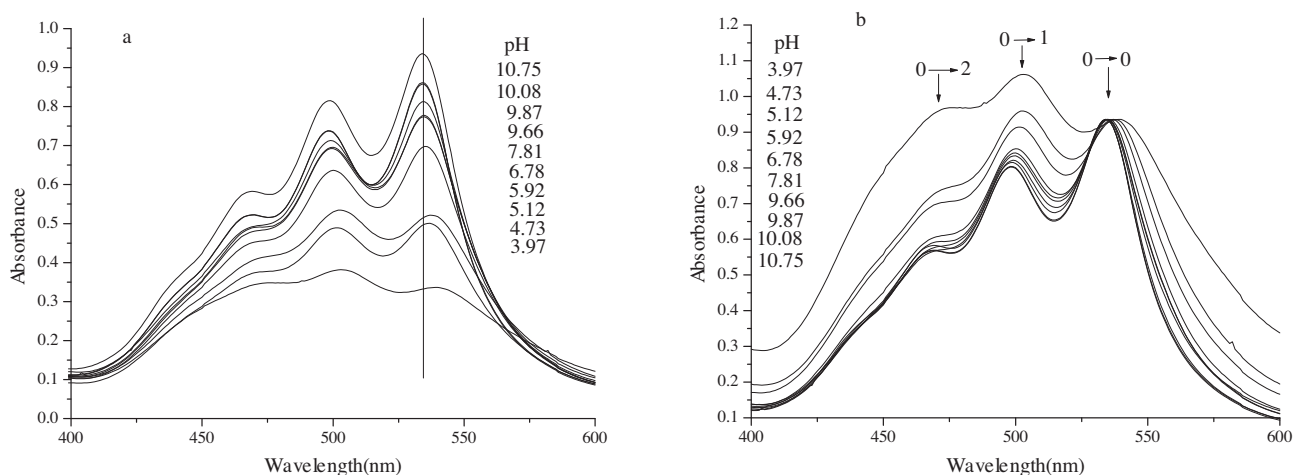

Scheme. Synthesis route of GAPTCD.

Figure 1. (a) Absorption and (b) normalized absorption spectra of GAPTCD in aqueous solution with varied pH ($c_{GAPTCD} = 10^{-5}$ mol/L).

2.1.2. Fluorescence spectra of GAPTCD

The fluorescence intensities of GAPTCD were also dependent on pH. Therefore, the effect of pH on the fluorescence emission was also investigated (Figure 2a). The fluorescence spectrum exhibited strong fluorescence (λmax = 550 nm) with a Stokes shift of 16 nm in alkali aqueous solution.
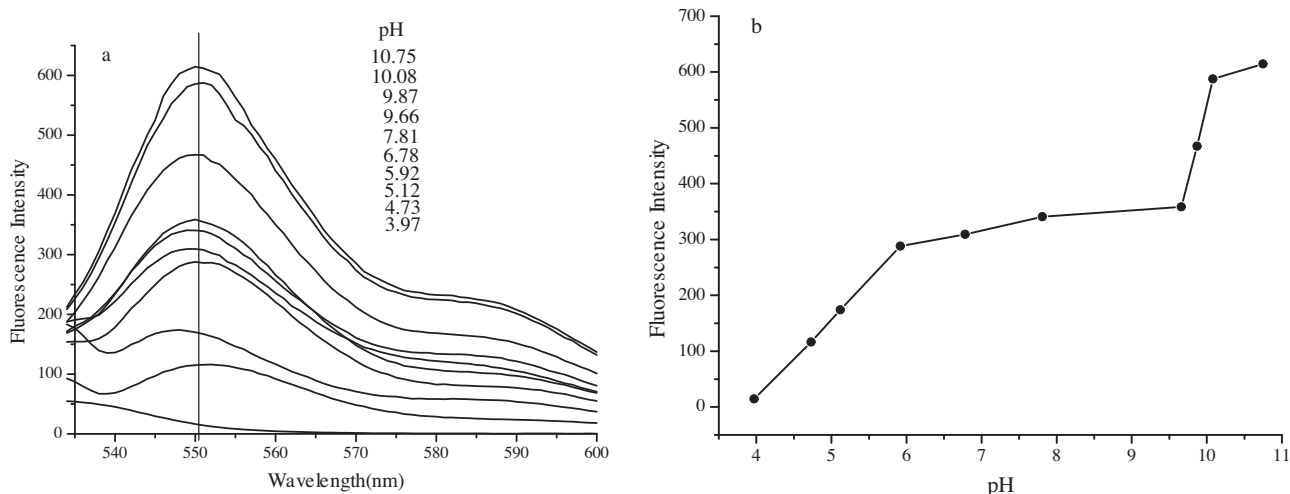

Figure 2. (a) Emission spectra of GAPTCD in aqueous solution with varied pH. (b) The corresponding graph with maximum fluorescence intensity and different pH, ($c_{GAPTCD} = 10^{-5}$ mol/L).

A rapid decline in fluorescence intensity was found upon a drop in pH from 10.75 to 9.66, while a steady reduction in fluorescence intensity was found upon a fall in pH from 9.66 to 5.92. The fluorescence of GAPTCD was quenched when the pH was inferior to 5.12. At pH 3.97 or lower, the fluorescence was completely quenched. GAPTCD showed strong fluorescence in basic and neutral solutions, but had little fluorescence in acidic solutions (Figure 2b). As a weak acid/weak base salt, GAPTCD was actually a neutral buffer exhibiting stability in a broad pH range from 5.92 to 9.87, which made it suitable for application in physiological conditions.

2.2. Electrostatic potential maps calculations

To clearly visualize the electronic properties of GAPTCD anion, molecular electrostatic potential maps (MEPs) were calculated with Gaussian03 installed on a Windows PC. For comparison purposes, compounds **2** and **3** were also calculated. Calculation of every part of the electron density cloud of the dyes was involved in the process. The MEP generated via this procedure was color-coded according to its potential with the most positive electrostatic potential shown in blue and those with the regions of most negative electrostatic potential shown in red. As shown in Figure 3, the regions with strong negative potential occurred in all of the molecules, suggesting a high negative electrostatic potential on the aromatic core.
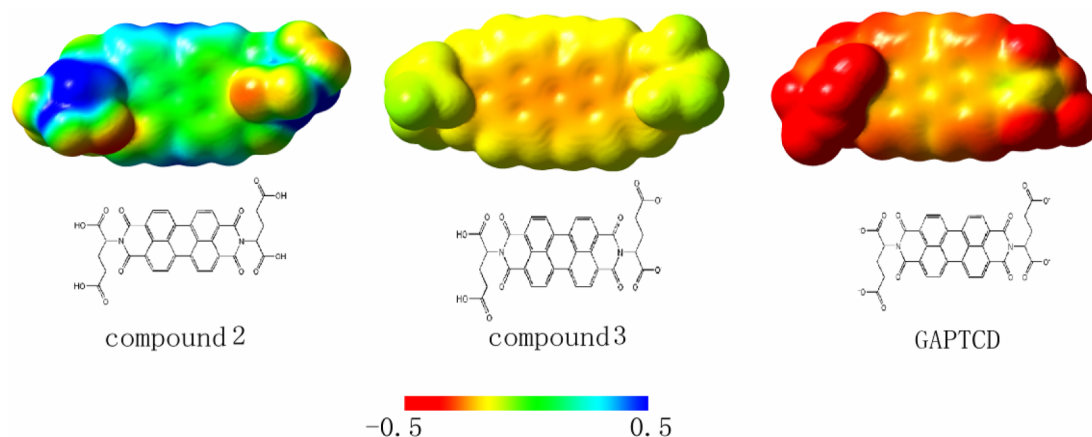

Figure 3. Electrostatic potential maps of GAPTCD and compounds **2** and **3** over an electronic isodensity of 0.0004e Å^{-3} at B3LYP/6-31G* level; the electron-rich regions are red and the electron-poor regions are blue.

High negative electrostatic potential increased electronic repulsion between GAPTCD monomers to lead to a high water-solubility of GAPTCD. The electrostatic potential of compound **3** was nearly neutral, indicating an even dispersion of the electrostatic potential. In contrast, the electrostatic potential of compound **2** molecule was completely positive, which resulted in $\pi - \pi$ stacking of the monomers. The MEP also suggested that GAPTCD can exist stably in basic to weak acidic aqueous solution.

2.3. Fluorescence imaging of living cells

The biological application of the probe GAPTCD was displayed through fluorescence imaging experiments and the studies were carried out with hela cells. Figure 4 shows the fluorescence images of hela cells stained with GAPTCD. In the absence of GAPTCD, it showed no detectable fluorescence signal in living cells (Figure 4a). After incubation with GAPTCD, a bright fluorescence from the cellular cytoplasm was observed in cells. These results suggested that GAPTCD can penetrate the cell membrane and accumulated in the cytoplasm (Figure 4b). After staining, the living hela cells appeared healthy as judged from their morphology, and they were devoid of any sign of structural degradation and vacuoles (Figure 4c).

In this paper, we presented the design, synthesis, spectroscopic properties, and biological evaluation of the glutamic functionalized water-soluble perylene diimide: GAPTCD (Scheme). High negative electrostatic potential increased electronic repulsion between GAPTCD monomers to lead to a high water-solubility of GAPTCD. The UV-vis and fluorescence spectra of GAPTCD suggested that it can exist stably in basic to weak acidic aqueous solution. Moieties with strong negative potential were present in all molecules, suggesting a high

negative electrostatic potential on the aromatic core. Optical imaging of GAPTCD in hela cells was further demonstrated. We think that water-soluble PDIs can also be an excellent candidate in biological systems.
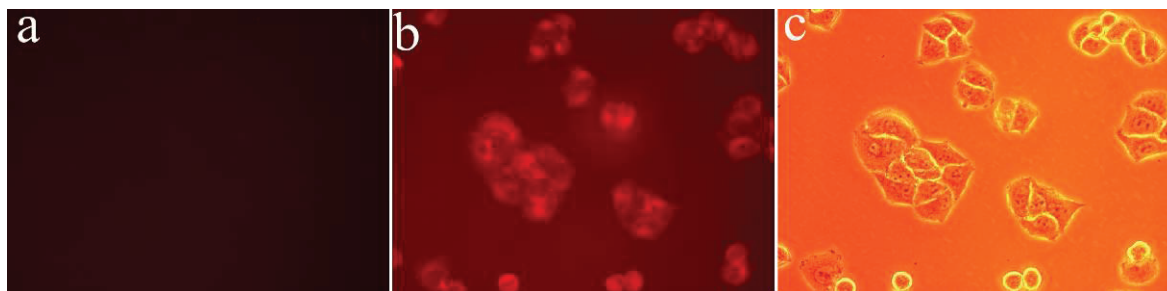

Figure 4. Fluorescence images of hela cells: (a) without GAPTCD. (b) Incubation with 10^{-5} M GAPTCD for 2.0 h and (c) Merged bright field images.

3. Experimental

3.1. Reagents and equipment

All reagents and solvents were analytical grade materials purchased from Beijing Chemical Corporation and used as obtained without further purification. GAPTCD was prepared in a similar way to the literature method.[11]

An INOVA 400-MHz spectrometer (Bruker, Germany) was used to record ^{1}H NMR and ^{13}C NMR. FT-IR spectra of samples mixed with KBr pellets were obtained through a TENSOR-27 Fourier transform spectrophotometer (Bruker, Germany). Mass spectra were taken on a Finnigan ESI instrument (Thermo, USA). UV-vis absorption spectra were performed on a CARY50 spectrophotometer (Varian, USA). Fluorescence spectra were carried out on a FL4500 PC spectrophotometer (Hitachi, Japan). Cells were observed and photographed on an Olympus (Japan) BH2 fluorescence microscope.

3.2. Synthesis of GAPTCD

L-glutamic acid (4.0 g, 24 mM), **1** (0.6 g, 1.6 mM), and 8.0 g of imidazole were mixed and heated to 165 °C for 7 h with stirring under N_2 atmosphere. After being cooled to room temperature, 100.0 mL of hot water was poured into the reaction flask, and then insoluble precipitate was filtered and discarded. To the aqueous solution was added 200 mL of 2.0 M diluted hydrochloric acid; then the precipitate was separated out and washed with water and ethanol, consecutively. The crude product was dissolved in 100.0 mL of DMF, and then diluted hydrochloric acid was added to adjust pH to $\sim$1. It was then dissolved in 100.0 mL of 0.1 M KOH solution and precipitated by adding diluted hydrochloric acid to pH $\sim$1. The precipitate was filtered and washed with diluted hydrochloric acid and ethanol. Compound **2** was then neutralized with 15 mL of 15% $NH_3 \cdot H_2O$ and stirred for 15 min. The precipitate was filtered off as solvent being evaporated and then dried under vacuum at 100 °C to give the reddish-brown product of GAPTCD (0.7 g, 72%). FT-IR (cm^{-1}): v 3433, 3164, 3052, 2847, 1689, 1592, 1361, 1345, 1273, 1182, 1114, 1021, 951, 853, 809, 793, 737, 659, 461, 432. ^{1}H NMR (D$_2$O, TMS, ppm): δ_H 8.38 (d, $J = 14.8$ Hz, 4H), 8.16 (d, $J = 15.0$ Hz, 4H), 6.32 (t, $J = 14.5$ Hz, 2H), 2.69–2.56 (m, 4H), 2.45–2.20 (m, 4H) (Figure 5). ^{13}C NMR (100 MHz, D$_2$O) 179.26, 177.03, 163.65, 138.28, 133.90, 133.38, 130.01, 126.52, 118.60, 55.17, 31.84, 23.61 (Figure 6). MS (MALDI-TOF): (m/z): 650.7 ([M + H]$^+$, calc. 650.12) (Figure 7).
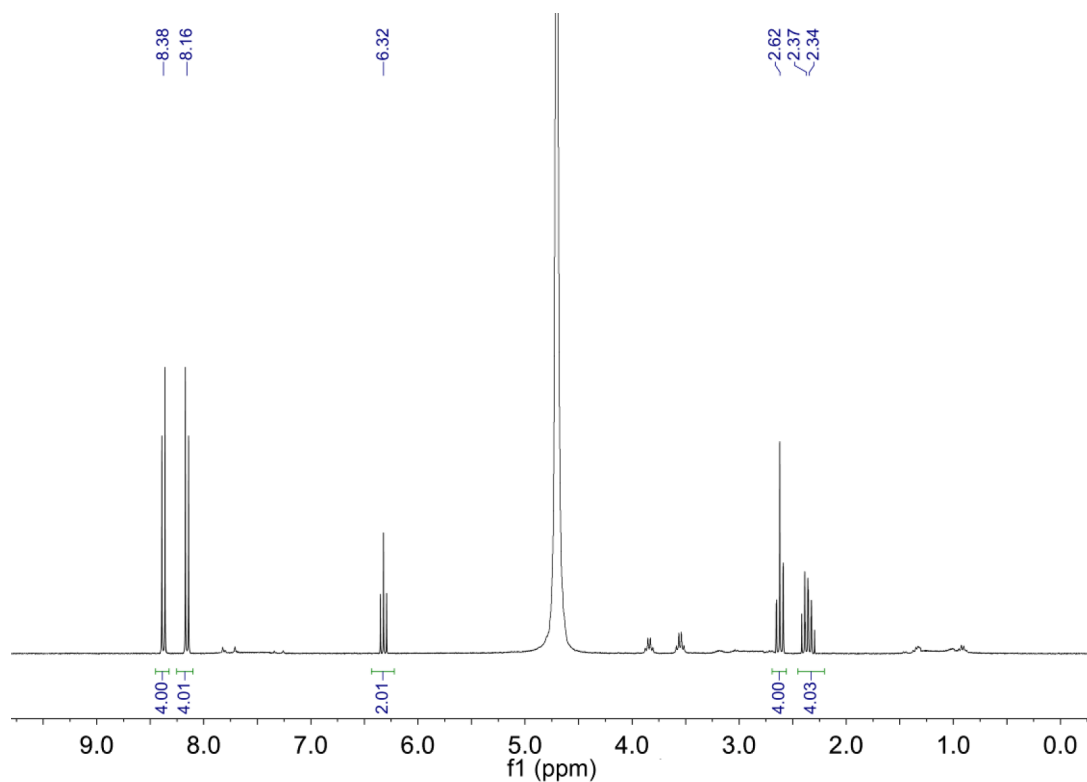
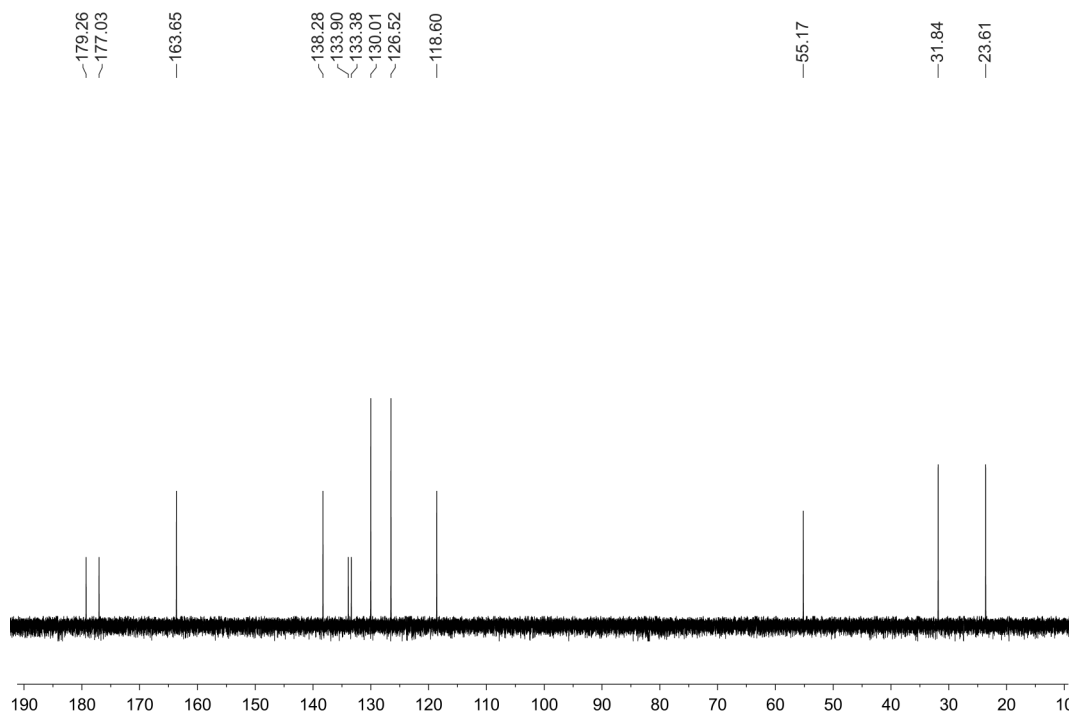**Figure 5.** ^{1}H NMR spectrum of GAPTCD.

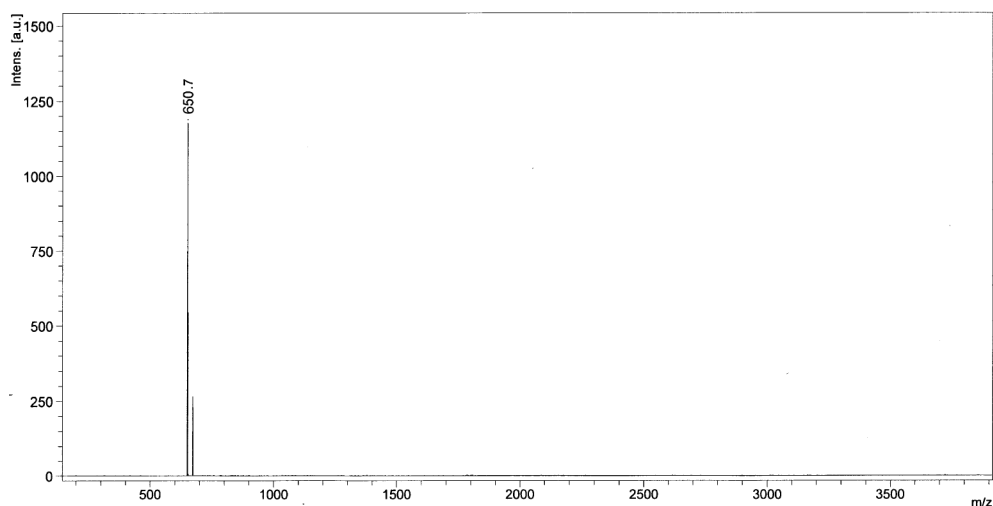**Figure 6.** ^{13}C NMR spectrum of GAPTCD.

Figure 7. MS (MALDI-TOF) spectrum of GAPTCD.

3.3. Cell culture for hela cells

Cervical cancer cells (hela cells) were cultured in high-glucose Dulbecco's modified Eagle's medium (DMEM, Sigma) containing 10% fetal bovine serum (FBS, Sigma), 100 μg/mL streptomycin (Sigma), 100 μg/mL penicillin (Sigma), and 5% CO_2 at 37 °C in an incubator. After 48 h of growth, the cells were subjected to 10 μM GAPTCD in water. Two hours later, the samples were viewed under the fluorescence microscope at an excitation with a UV-filter source of 330–380 nm.

Acknowledgments

References

1. Peneva, K.; Mihov, G.; Herrmann, A.; Zarrabi, N.; Börsch, M.; Duncan, T. M.; Müllen, K. *J. Am. Chem. Soc.* **2008**, *130*, 5398–5399.

2. Che, Y.; Yang, X.; Zang, L. *Chem. Commun.* **2008**, 1413–1415.

3. Chen, X.; Jou, M. J.; Yoon, J. *Org. Lett.* **2009**, *11*, 2181–2184.

4. Bin, W.; Cong Y. *Angew. Chem., Int. Ed.* **2010**, *49*, 1485–1488.

5. Szekle, H.; Schübel, S.; Harenberg, J.; Krämer, R. *Chem. Commun.* **2010**, *46*, 1667–1669.

6. Avlasevich, Y.; Li, C.; Müllen, K. *J. Mater. Chem.* **2010**, *20*, 3814–3826.

7. Demmig, S.; Langhals, *H. Chem. Ber.* **1988**, *121*, 225–230.

8. Holtrup, F. O.; Müller, H.; Quante, S.; De Feyter, F. C.; Schryver, D.; Müllen, K. *Chem. Eur. J.* **1997**, *3*, 219–225.

9. Yukruk, F. A.; Lale D.; Canpinar, H.; Dicle G.; Engin U. *Org. Lett.* **2005**, *7*, 2885–2287.

10. Weil, T.; Reuther, E.; Beer C.; Müllen, K. *Chem. Eur. J.* **2004**, *10*, 1398–1414.

11. Zhong L.; Xing F.; Shi W.; Yan L.; Xie L.; Zhu S. *Appl. Mater. Interfaces* **2013**, *5*, 3401–3407.

12. Würthner, F. *Chem. Commun.* **2004**, 1564–1579.

13. Chen, Z.; Stepanenko, V.; Dehm, V.; Prins, P.; Seibbeles, L. D. A.; Seibt, J.; Marquetand, P.; Engel, V.; Würthner, F. *Chem. Eur. J.* **2007**, *13*, 436–449.

14. Ji, H.; Majithia, R.; Yang, X.; Xu, X.; More, K. *J. Am. Chem. Soc.* **2008**, *130*, 10056–10057.

15. Araújo, R.; Silva, C.; Paiva, M.; Franco, M.; Proença, M. *RSC Adv.* **2013**, *3*, 24535–24542.

16. Gao, B.; Li, H.; Liu, H.; Zhang, L.; Bai, Q.; Ba, X. *Chem. Commun.* **2011**, *47*, 3894–3896.

17. Jiang, X.; Lo, P.; Yeung, S.; Fong, W.; Ng, D. K. P. *Chem. Commun.* **2010**, *46*, 3188–3190.

18. Yin, M.; Shen, J.; Pflugfelder, G. O.; Weil, T.; Müllen, K. *J. Am. Chem. Soc.* **2008**, *130*, 7806–7807.

19. Ma, Y.; Wang, C.; Zhao, Y.; Yu, Y.; Han, C.; Qiu, X.; Shi, Z. *Supramol. Chem.* **2007**, *19*, 141–149.

20. Langhals, H.; Ismael, R. *Eur. J. Org. Chem.* **1998**, *9*, 1915–1917.